The International Journal of Energy & Engineering Sciences, 2021, 6 (1) 1-12
ISSN: 2602-294X - Gaziantep University

THERMAL FATIGUE RESISTANCE OF GLASS/EPOXY LAMINATED COMPOSITES

Mert Kesikminare[1], Eyüp Yeter[2,*]

[1]Aerospace Engineering Dept., Aeronautics and Aerospace Faculty, Gaziantep University, Gaziantep, Turkey.
[2]Aerospace Engineering Dept., Aeronautics and Aerospace Faculty, Gaziantep University, Gaziantep, Turkey.

[*]eyeter@gantep.edu.tr

ABSTRACT

The material of the fiber and matrix of polymer matrix composites directly influences the mechanical performance of a composite. Fibers are generally expected to have high elastic modulus and strengths. Due to the nature of polymer matrix composites, due to the combination of different materials at the macroscopic level, they are highly affected by thermal loads. Sometimes, perhaps the most important design criterion may be the resistance of these materials to thermal loads. Also, these loads can be repeated due to the needs of usage areas. Especially in the aviation industry, resistance to repetitive thermal loads is very important in the design of aerospace vehicles. In this study, it is aimed to understand the behavior of Glass/Epoxy polymer matrix composites under thermal fatigue loads. $[(0/90)_2]_s$, $[(15/-75)_2]_s$, $[(30/-60)_2]_s$, and $[(45/-45)_2]_s$ fiber orientations are used. Effects of two different boundary conditions are also researched.

Keywords: Polymer Composites, Thermal fatigue, FEM.

1. INTRODUCTION

Today's engineering has evolved to design structures resistant to different types of loads and to develop materials suitable for these designs. Polymer matrix composites have become the most important choice for researchers with their many superior features. Especially, high specific modulus and strength, and dimensional stability during large changes in temperature in space make the polymer matrix composites the material of choice in space applications. However, composite materials have some disadvantages besides their superior properties. The strength of composite materials against repeated loads is important in this context and has been investigated by many researchers. Thermal fatigue can be defined as the exposure of structures or materials to repeated thermal loads. These thermal loads can be above zero degrees, below zero degrees, or a temperature below zero to a temperature above zero. For instance, satellite structures should be dimensionally stable in space during temperature changes between –165 °C and 100 °C. Yeter [1,2] has worked on the effects of thermal

fatigue on the 2014, 2024, 6061, and 7075 aluminum alloys, which are mostly used in the aviation industry. An algorithm was developed on the ANSYS program so that it has the opportunity to examine the behavior of materials subjected to repeated thermal loads. Yeter and Ozer [3] studied on thermal fatigue characteristics of Plates with Cutouts. In this study, using aluminum alloys square plate circular, triangular, elliptical, and square cutouts opened on the square plate. Kobayashi et al. [4,5] conducted thermal fatigue experiments on carbon fiber reinforced plastics cross-ply to obtain damages that influence the mechanical properties of the composite. Zhou et al [6] investigated the resistance of the molybdenum plate containing Al_2O_3 particles under the cyclic thermal loads. The thermal fatigue life of ZrB2-SiC-graphite composite at ultrahigh temperatures was researched by Chen et al. [7]. The thermal shock and thermal fatigue behaviors of monolithic Si3N4 nano-ceramic and Si3N4–TiC nano-composites were investigated through the water-quench method by Tian et al [8]. Misak et al. [9] investigated Thermal fatigue resistance of carbon nanotube wires. Gkikas et al. [10] studied the behaviors of CNTs under the hydrothermal and thermal shock loads. Göv [11] performed a study to develop an algorithm to design the layer and fiber number of the composite plate. stress values were used to determine fiber angle and maximum stress failure theory was used to obtain layer numbers. Dogru [12] developed an algorithm to Design Optimization of laminated structures using TsaiWu criteria.
In this study, the thermal fatigue behavior of Glass/epoxy composites has been investigated numerically. $[(0/90)_2]_s$, $[(15/-75)_2]_s$, $[(30/-60)_2]_s$, and $[(45/-45)_2]_s$ fiber orientations are used. Effects of two different boundary conditions are also researched. Also, the effects of the stress concentration are investigated by opening circular cut-outs.

2. MATERIALS and METHODS

In this study, the thermal fatigue resistance of Glass/Epoxy laminated composites under the thermal fatigue loading has been investigated. The algorithm previously created by Yeter [1,2] has been adopted on composite materials. The used material properties are shown in Table 1.

Table 1. Mechanic properties of Glass/Epoxy [13]

Property	Units	Value
Fiber volume fraction		0.45
Longitudinal elastic modulus (E1)	GPa	38.6
Transverse elastic modulus (E2)	GPa	8.27
Major Poisson's ratio (ν_{12})		0.26
Shear Modulus (G_{12})	GPa	4.14
Ultimate longitudinal tensile strength	MPa	1062
Ultimate longitudinal compressive strength	MPa	610
Ultimate transverse tensile strength	MPa	31
Ultimate transverse compressive strength	MPa	118
Ultimate in-plane shear strength	MPa	72

The flow chart used in this algorithm is given in Figure 3.1. This algorithm is based on the principle of determining the factor of safety of the material subjected to the thermal fatigue

load. The Soderberg failure theory was used in this study and factor of safety formulation is given as;

$$n = \frac{1}{\frac{S_a}{S_e} + \frac{S_m}{S_y}} \quad (1)$$

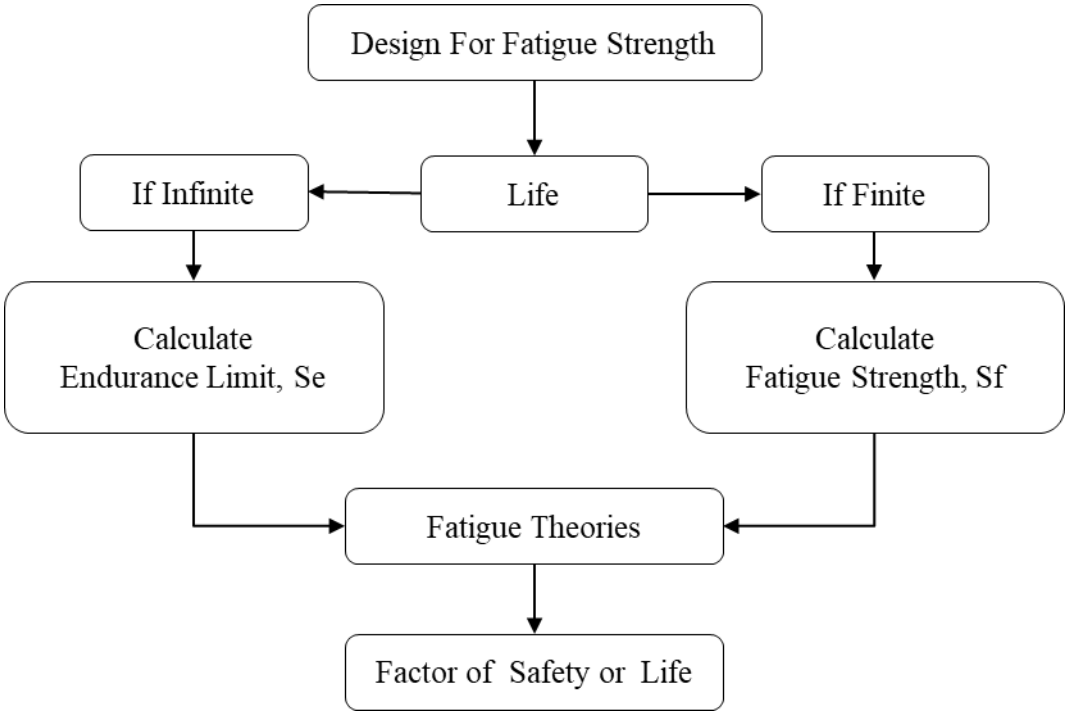

Figure 1. Flowchart for the design for fatigue strength

The SHELL181 element type is used that is used for layered applications to model laminated composites. The accuracy of the composite model is governed by the first-order shear deformation theory. The element kinematics allow for finite membrane strains (stretching). However, the curvature changes within a time increment are assumed to be small. The used plate dimensions are taken as constant and these dimensions are 100 mm length, 50 mm width. Each layer thickness is taken as 0.25 mm. +100°C uniform temperature load was applied and then the plate subjected to -130°C thermal load. The reference temperature was taken as 25 C° in fatigue cycles. The boundary conditions given in Figure 1 are used. As seen in this figure, all edges of the plate are fixed (fix-all) and left and right edge fixed (fix-fix) boundary conditions are considered.

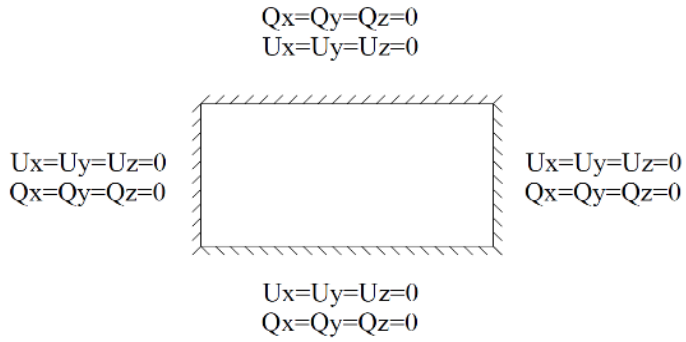

(a)

(b)

Figure 2. Boundary condition, (a) fix-all and (b) fix-fix

3. RESULTS AND DISCUSSIONS

Safety factor distributions of Glass/Epoxy fiber reinforced composites under the thermal fatigue loads are given in this section. Results of thermal fatigue load for different fiber orientations $[(0/90)_2]_s$, $[(15/-75)_2]_s$, $[(30/-60)_2]_s$, and $[(45/-45)_2]_s$ are given. The factor of safety distribution for fix-all boundary conditions under pure thermal fatigue load for $[(0/90)_2]_s$ are compared for Glass/Epoxy.

Factor of safety distribution for fix-all and fix-fix boundary conditions under pure thermal fatigue load for $[(0/90)_2]_s$ ply sequences are given in Figure 3. The figure shows that the plate has the same factor of safety for all points for all-fix boundary conditions. But for the fix-fix condition, the safety factor values vary from point to point and the minimum safety value for fix-fix is less than the fix-all boundary conditions. Also, Figures 4 and 5 presents the variation of the lowest factor of safety with respect to different fiber orientations and ply sequences. As seen in these figures, for fix-fix boundary conditions fiber orientations have direct effects safety factor value of laminates. $[(0/90)_2]_s$ ply sequence has the highest safety factor and $[(45/-45)_2]_s$ has the lowest safety factor value. The safety factor values of $[(15/-75)_2]_s$ and $[(30/-60)_2]_s$ are between $[(0/90)_2]_s$ and $[(45/-45)_2]_s$ ply sequences.

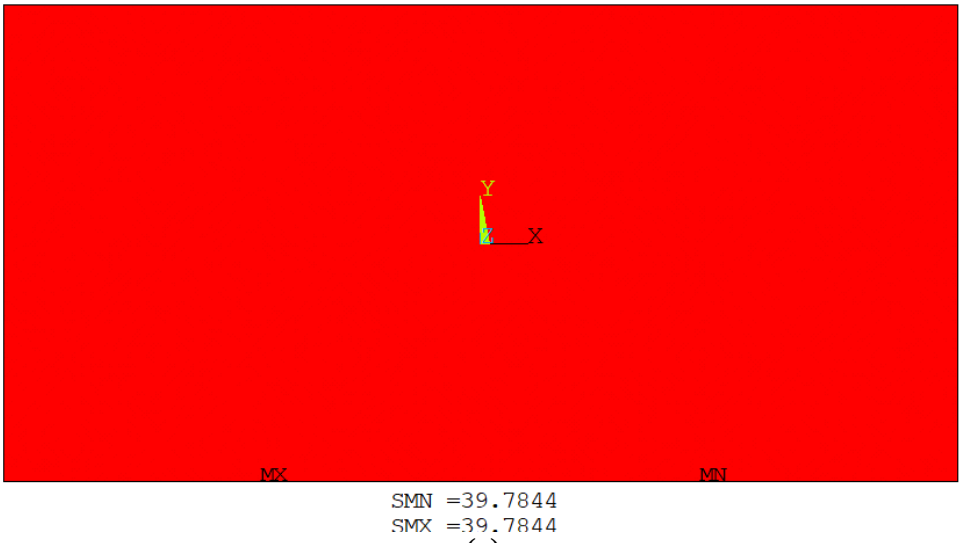

(a)

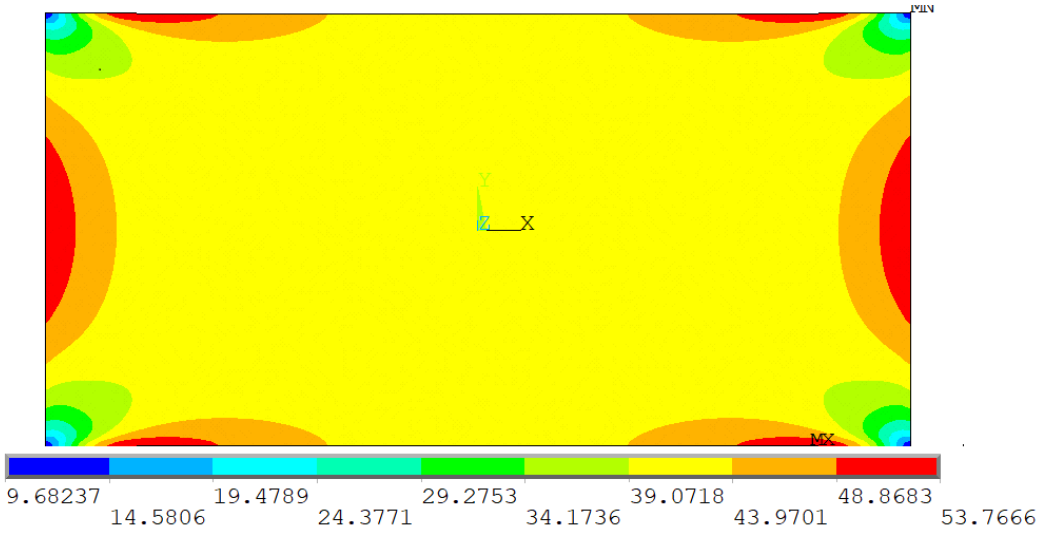

(b)

Figure 3. The factor of safety for fix-all boundary condition under pure thermal fatigue for $[(0/90)_2]_s$ orientation for different boundary conditions (a) Fix-all, (b) Fix-fix

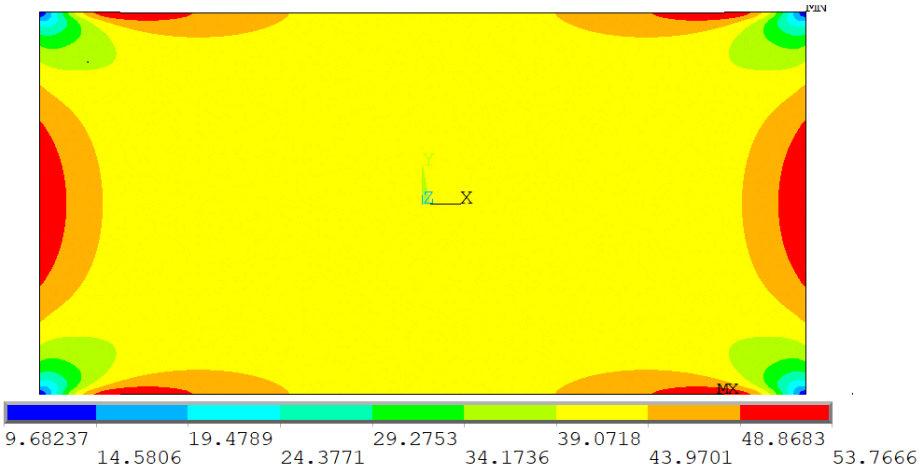
MN
Y
Z
X
MX
9.68237
14.5806
19.4789
24.3771
29.2753
34.1736
39.0718
43.9701
48.8683
53.7666

(a)

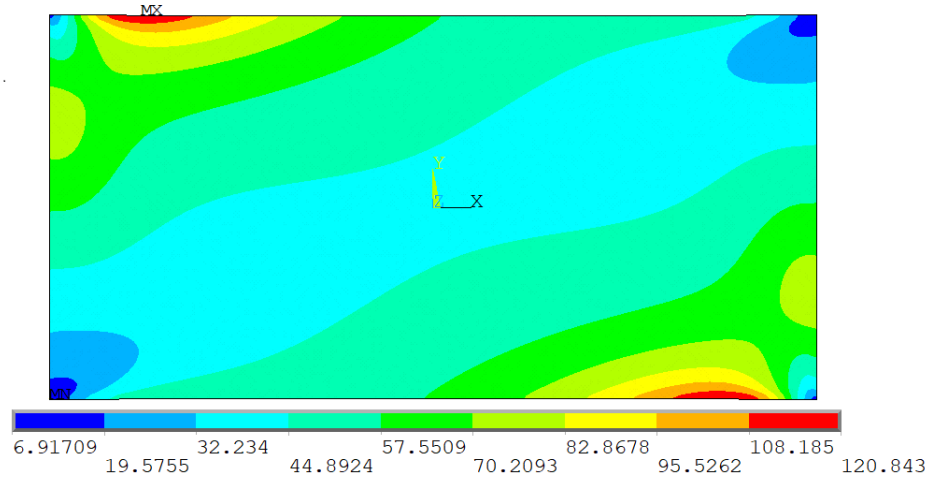
MX
Y
Z
X
MN
6.91709
19.5755
32.234
44.8924
57.5509
70.2093
82.8678
95.5262
108.185
120.843

(b)

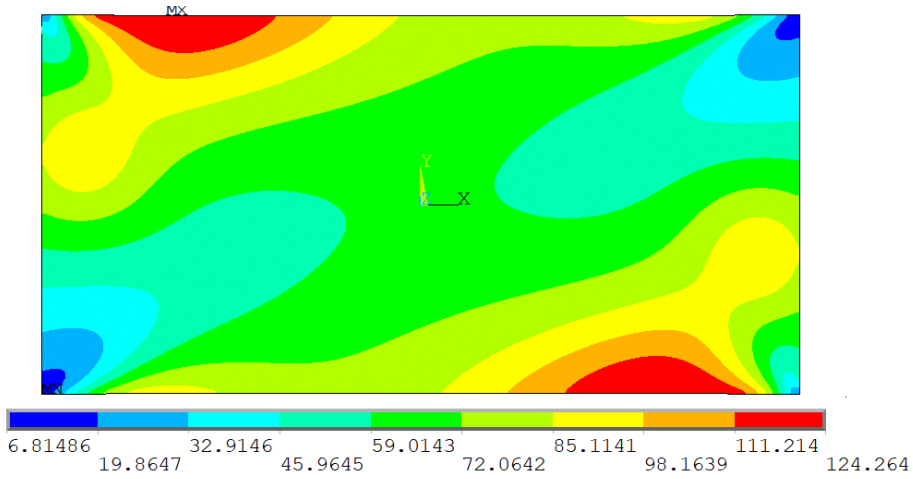
MX
Y
Z
X
MN
6.81486
19.8647
32.9146
45.9645
59.0143
72.0642
85.1141
98.1639
111.214
124.264

(c)

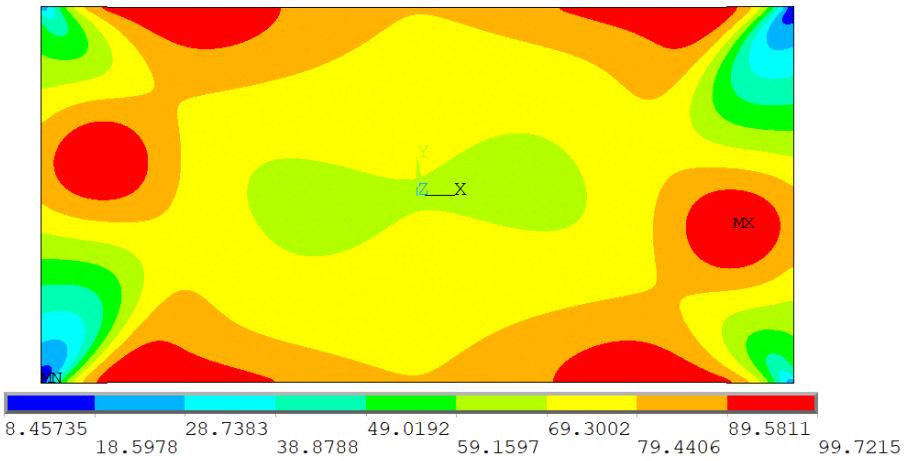

(d)

Figure 4. Safety factor distribution of Glass/Epoxy for fix-fix boundary condition at different fiber orientations (a) $[(0/90)_2]_s$, (b) $[(15/-75)_2]_s$, (c) $[(30/-60)_2]_s$, (d) $[(45/-45)_2]_s$

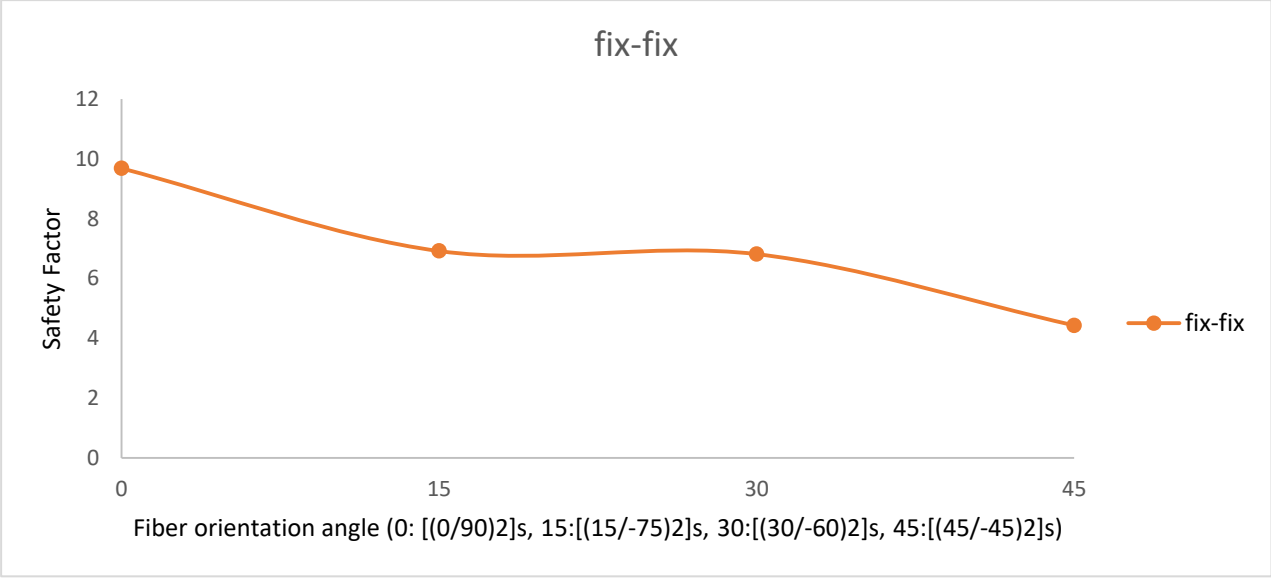

(a)

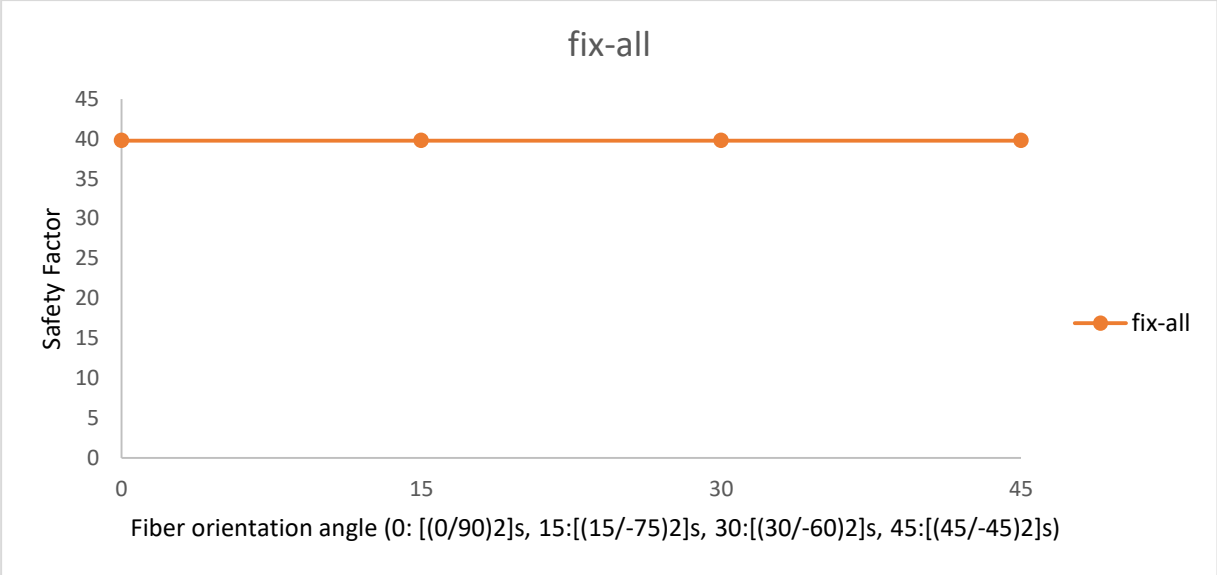

(b)

Figure 5. Variation of the safety factor of Glass/Epoxy with Fiber orientation angle for different boundary conditions (a) Fix-Fix, (b) Fix-all

The behavior of polymer matrix composites under the thermal fatigue loads that contain different cut-outs is presented. The cut-outs are opened to see the effects of stress concentration on the thermal fatigue resistance of the fiber reinforced composites.
Figures 6 and 7 shows safety factor values for Glass/Epoxy $[(0/90)_2]_s$ fiber orientation with circular cutout for fix-fix boundary condition under pure thermal fatigue with different cutout sizes. As seen in the figure the minimum safety factor value for the circular cutout is increased by nearly 13.4 % when the cutout size (A) is increased 30 mm from 10 mm.

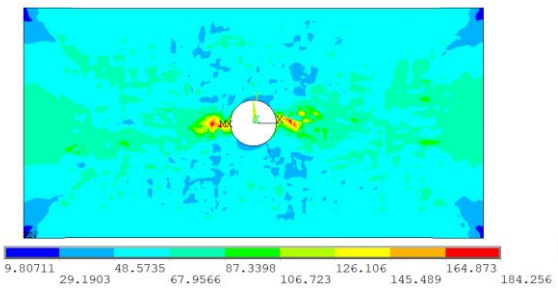

(a)

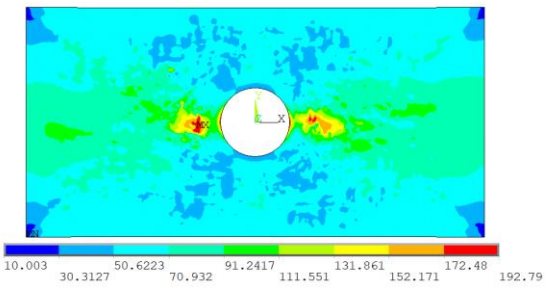

(b)

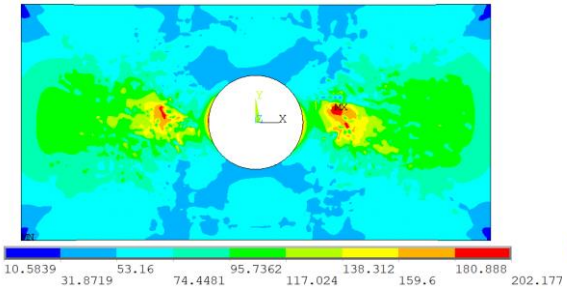

(c)

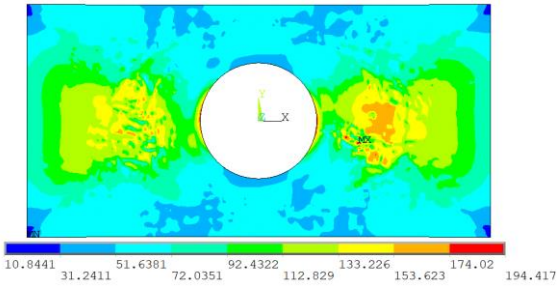

(d)

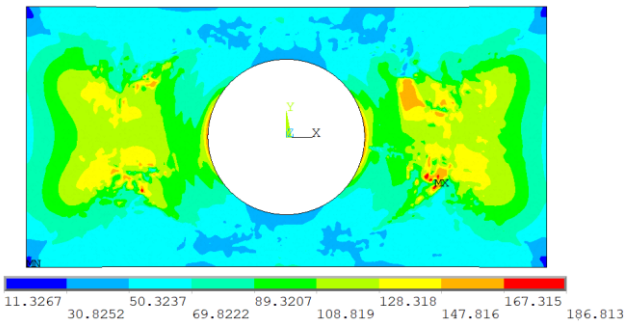

(e)

Figure 6. Safety factor distribution of Glass/Epoxy $[(0/90)_2]_s$ fiber orientation with a circular cutout for fix-fix boundary condition under pure thermal fatigue with different cutout sizes (a)10, (b)15, (c)20, (d)25, (e) 30

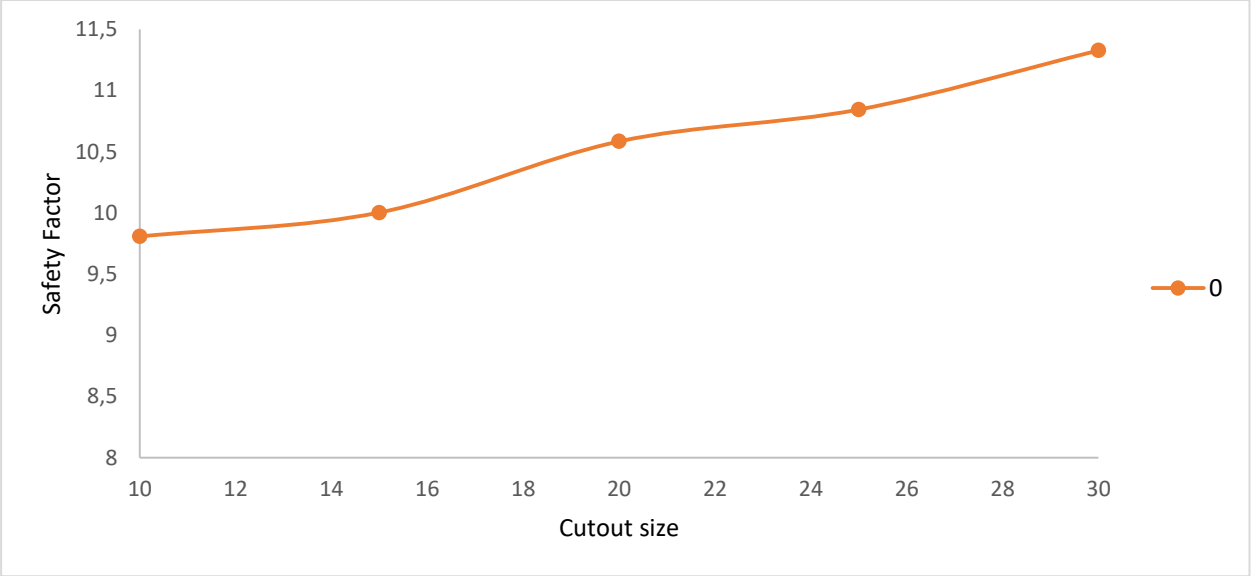

Figure 7. Variation of Glass/Epoxy $[(0/90)_2]_s$ fiber orientation with a circular cutout for fix-fix boundary condition

Safety factor distribution of Glass/Epoxy with $[(0/90)_2]_s$ fiber orientation for circular 20 mm cut-out and with different cutout positions are given in Figures 8 and 9. As seen in the figures, the factor of safety has the highest value when cut-out is at the center. When the cutout is positioned on the left and right sides of the center, the safety factor value is minimum.

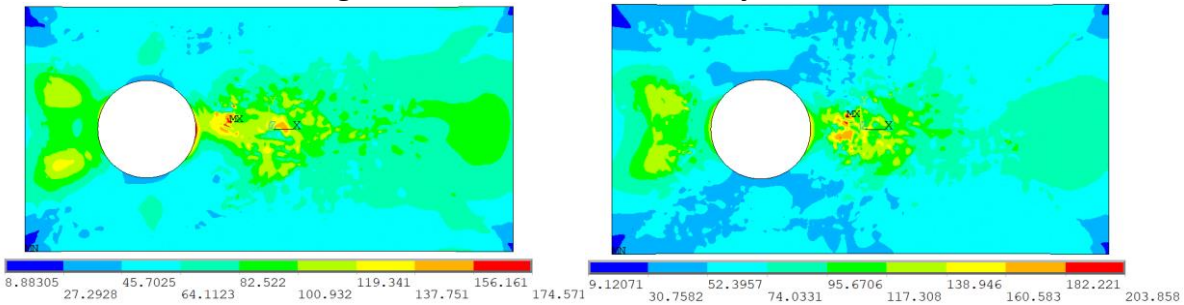

(a) (b)

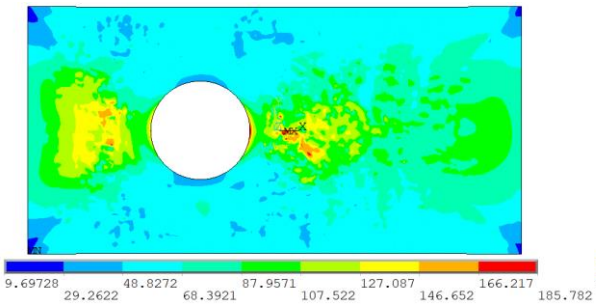
9.69728
29.2622
48.8272
68.3921
87.9571
107.522
127.087
146.652
166.217
185.782

(c)

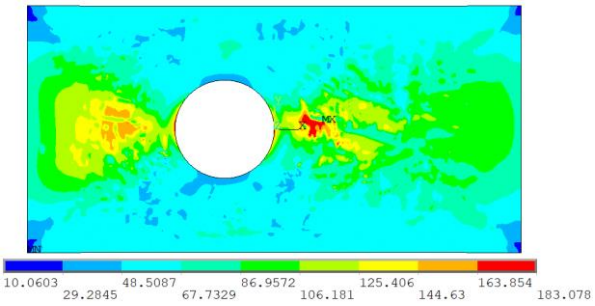
10.0603
29.2845
48.5087
67.7329
86.9572
106.181
125.406
144.63
163.854
183.078

(d)

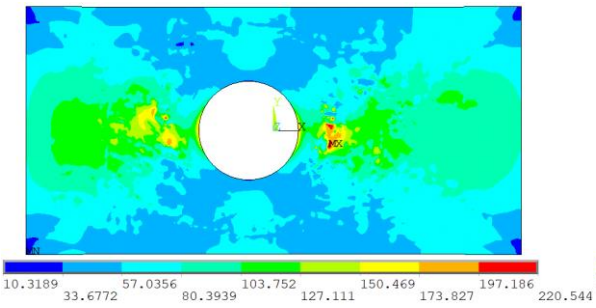
10.3189
33.6772
57.0356
80.3939
103.752
127.111
150.469
173.827
197.186
220.544

(e)

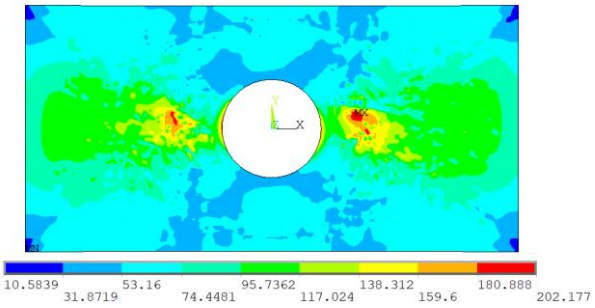
10.5839
31.8719
53.16
74.4481
95.7362
117.024
138.312
159.6
180.888
202.177

(f)

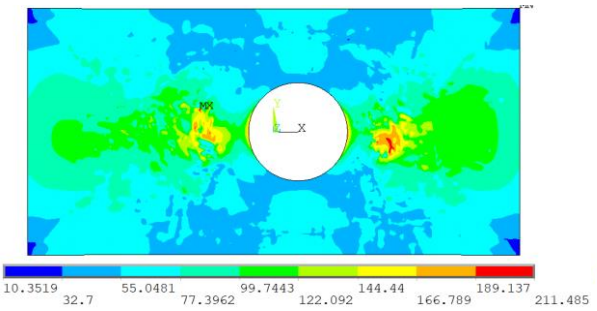
10.3519
32.7
55.0481
77.3962
99.7443
122.092
144.44
166.789
189.137
211.485

(g)

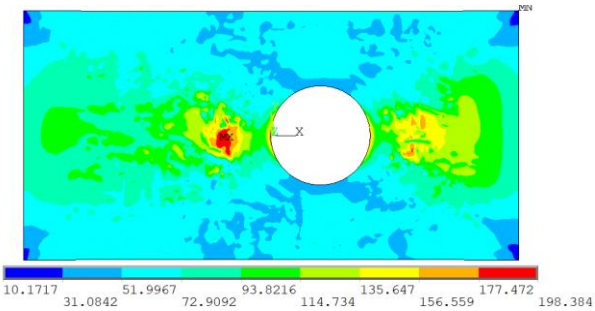
10.1717
31.0842
51.9967
72.9092
93.8216
114.734
135.647
156.559
177.472
198.384

(h)

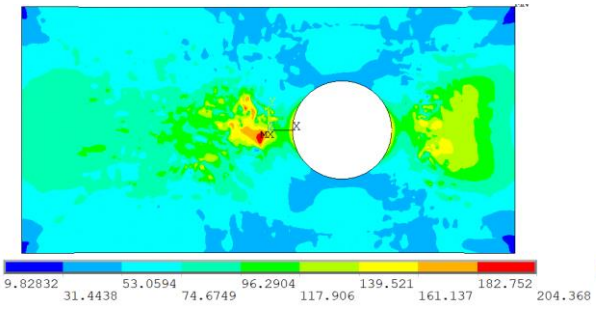
9.82832
31.4438
53.0594
74.6749
96.2904
117.906
139.521
161.137
182.752
204.368

(i)

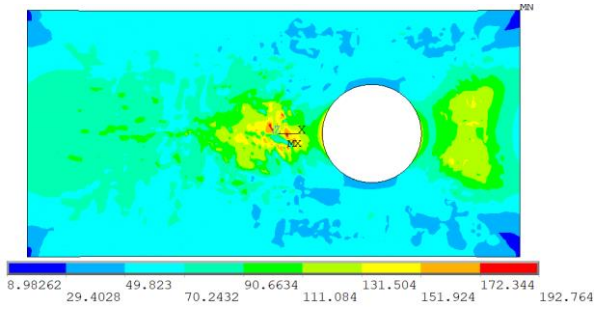
8.98262
29.4028
49.823
70.2432
90.6634
111.084
131.504
151.924
172.344
192.764

(j)

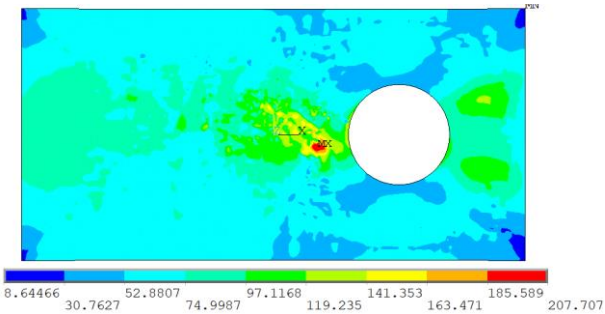
8.64466
30.7627
52.8807
74.9987
97.1168
119.235
141.353
163.471
185.589
207.707

(k)

Figure 8. Safety factor distribution of Glass/Epoxy with $[(0/90)_2]_s$ fiber orientation with fix-fix boundary conditions for circular 20 mm cut-out and with different cut-out positions (a)-25, (b) -20, (c) -15, (d)-10, (e) -5, (f) 0, (g) 5, (h)10, (i)15, (j) 20, (k) 25

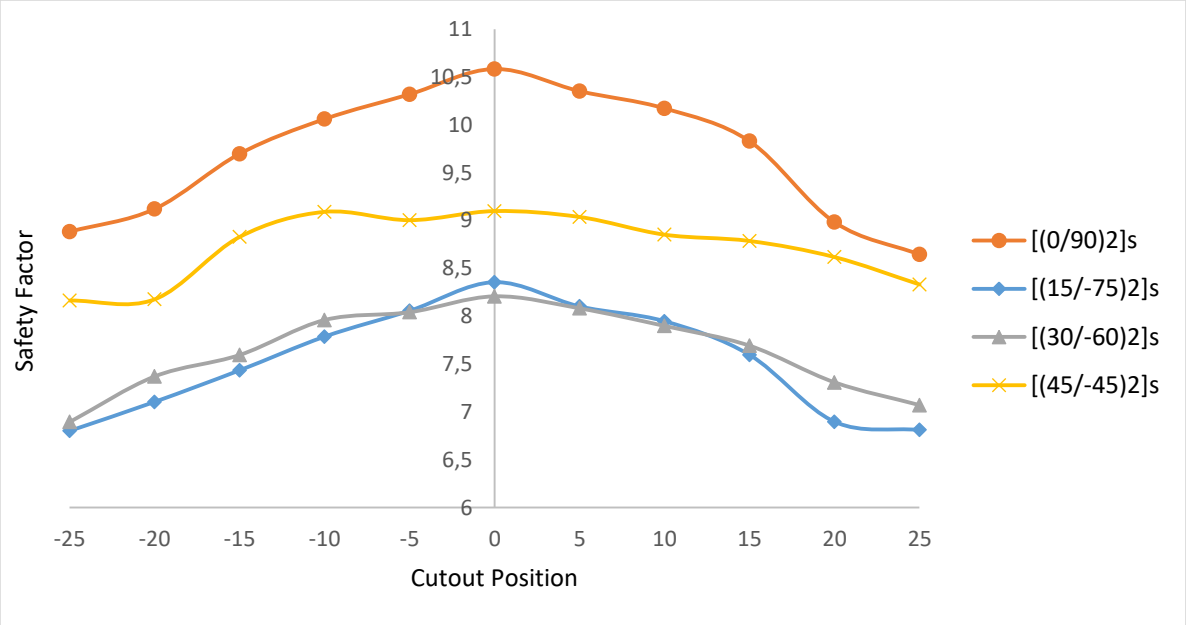

Figure 9. Variation of the safety factor of Glass/Epoxy with $[(0/90)_2]_s$ fiber orientation with fix-fix boundary conditions for circular 20 mm cut-out and with different cutout positions

CONCLUSIONS

The thermal fatigue behavior of Glass/Epoxy composites has been investigated numerically. $[(0/90)_2]_s$, $[(15/-75)_2]_s$, $[(30/-60)_2]_s$, and $[(45/-45)_2]_s$ fiber orientations are used. Effects of two different boundary conditions are also researched. It is s seen that fiber orientation and boundary conditions directly affect the thermal fatigue resistance. $[(0/90)_2]_s$, ply sequence has the highest safety factor, and $[(45/-45)_2]_s$ has the lowest safety factor value. The safety factor values of $[(15/-75)_2]_s$, and $[(30/-60)_2]_s$ are between $[(0/90)_2]_s$ and $[(45/-45)_2]_s$ ply sequences. Also, the circular cut-outs are opened to see the effects of stress concentration on the thermal fatigue resistance of the fiber-reinforced composites.

The minimum safety factor value for the circular cutout is increased by nearly 13.4 % when the cutout size (A) is increased 30 mm from 10 mm. The factor of safety has the highest value when cut-out is at the center. When the cutout is positioned on the left and right sides of the center, the safety factor value is minimum.

REFERENCES

[1] Yeter, Eyüp. (2018). Thermal Fatigue Analyses of Riveted Structures. Mechanics. 24.5: 689-694

[2] Yeter, Eyüp. (2018). Thermal fatigue characteristics of materials used in aerospace structures. Energy, Ecology and Environment. 3.1: 24-31.

[3] Yeter E and Özer L. Thermal Fatigue Characteristics of Plates with Cutouts. International Advanced Researches Engineering Congress-2017.

[4]Kobayashi, S., Terada, K., Ogihara, S., & Takeda, N. (2001). Damage-mechanics analysis of matrix cracking in cross-ply CFRP laminates under thermal fatigue. Composites science and technology, 61(12), 1735-1742.

[5] Kobayashi, S., Terada, K., & Takeda, N. (2003). Evaluation of long-term durability in high temperature resistant CFRP laminates under thermal fatigue loading. Composites Part B: Engineering, 34(8), 753-759.

[6] Zhou, Y., Wei, S., Wang, L., Xu, L., Li, X., & Pan, K. (2020). Study on thermal fatigue performance of the molybdenum plate doped with Al2O3 particles. Journal of Alloys and Compounds, 823, 153748.

[7] Chen, X., Peng, X., Wei, Z., Yue, X., & Fu, T. (2017). Effect of tensile stress on thermal fatigue life of ZrB2-SiC-graphite composite. Materials & Design, 126, 91-97.

[8] Tian, C., Liu, N., & Lu, M. (2008). Thermal shock and thermal fatigue behavior of Si3N4–TiC nano-composites. International Journal of Refractory Metals and Hard Materials, 26(5), 478-484.

[9]Misak, H. E., Sabelkin, V., Mall, S., & Kladitis, P. E. (2013). Thermal fatigue and hypothermal atomic oxygen exposure behavior of carbon nanotube wire. Carbon, 57, 42-49.

[10] Gkikas, G., Douka, D. D., Barkoula, N. M., & Paipetis, A. S. (2015). Nano-enhanced composite materials under thermal shock and environmental degradation: a durability study. Composites Part B: Engineering, 70, 206-214.

[11] Göv, İ., "A novel approach for design of fiber angle and layer number of composite plates", Polymer Composites, 2017, 38(2): 268-276.

[12]Doğru, M.H., "Tsai-wu kriteri kullanarak kompozit plakaların optimizasyonu için geliştirilen algoritma", Journal of the Faculty of Engineering and Architecture of Gazi University, 32(3): 821-829, (2017).

[13] Kaw, A. K. (2005). Mechanics of composite materials. CRC press.